Inorg. Chem. **2007**, *46*, 4844–4849

Inorganic Chemistry
Article

# Multiple Bismuth(III)–Thioether Secondary Interactions Integrate Metalloporphyrin Ligands into Functional Networks

**Kunhao Li,[†] Guo Huang,[‡] Zhengtao Xu,*,[‡] Mingliang Zhang,[‡] Matthias Zeller,[§] Allen D. Hunter,[§] Stephen Sin-Yin Chui,[||] Chi-Ming Che,[||] and Wai-Yeung Wong[⊥]**

*Department of Chemistry, The George Washington University, 725 21st Street NW, Washington, D.C. 20052, Department of Biology and Chemistry, City University of Hong Kong, 83 Tat Chee Avenue, Kowloon, Hong Kong, China, Department of Chemistry, Youngstown State University, One University Plaza, Youngstown, Ohio 44555, Department of Chemistry, The University of Hong Kong, Pokfulam Road, Hong Kong, China, and Department of Chemistry, Hong Kong Baptist University, Waterloo Road, Kowloon Tong, Hong Kong, China*

Received September 10, 2006

We introduce the 1,2,3-tris(organylthiophenyl) group as a symmetrical, multidentate chelation link for building coordination networks. For this, zinc(II) 5,10,15,20-tetrakis[3′,4′,5′-tris(methylthio)phenyl]porphyrin was synthesized and integrated into a two-dimensional network via coordination with $BiBr_3$. The coordination link exhibits an unusually complex bonding pattern, involving six S atoms from two neighboring ligands that form multiple Bi–S interactions (distances ranging from 3.08 to 3.63 Å) with a dimerlike unit of $Bi_2Br_6$. The electronic interaction between the porphyrin center and the $Bi_2Br_6$ block was illustrated by the diffuse-reflectance spectrum of the network compound, in which a modest red-shifted feature at 1.8 eV was seen (while the Q-band absorption of the metalloporphyrin core continues to be dominant at 1.9 eV).

## Introduction

In the growing field of coordination networks,[1−5] it is of interest to develop ligand systems for uncovering novel structural features (e.g., local coordination bonding patterns and network connectivity) and for achieving richer functionalities in the solid state. Among the numerous considerations, ligand symmetry and chelation ability are two features that could offer important advantages. Besides the general aesthetic appeal, rigid, symmetrical ligands tend to facilitate the formation of highly ordered, crystalline extended networks,[6−13] apparently because the multiple equivalent positions allow the ligand to achieve more readily the required orientation in the growing lattice. On the other hand, chelation bonds attract attention as linkages for extended networks,[14−19] partly because of the potentially higher bonding strength that might be achieved in comparison to single-fold coordination bonds. The discovery reported here arises from the newly synthesized porphyrin ligand zinc(II)

---

* To whom correspondence should be addressed. E-mail: zhengtao@cityu.edu.hk.
[†] The George Washington University.
[‡] City University of Hong Kong.
[§] Youngstown State University.
[||] The University of Hong Kong.
[⊥] Hong Kong Baptist University.

(1) Janiak, C. *Dalton Trans.* **2003**, 2781.
(2) James, S. L. *Chem. Soc. Rev.* **2003**, *32*, 276.
(3) Kesanli, B.; Lin, W. *Coord. Chem. Rev.* **2003**, *246*, 305.
(4) Batten, S. R.; Robson, R. *Angew. Chem., Int. Ed.* **1998**, *37*, 1461.
(5) Ockwig, N. W.; Delgado-Friedrichs, O.; O'Keeffe, M.; Yaghi, O. M. *Acc. Chem. Res.* **2005**, *38*, 176.
(6) Xu, Z.; Kiang, Y.-H.; Lee, S.; Lobkovsky, E. B.; Emmott, N. *J. Am. Chem. Soc.* **2000**, *122*, 8376.
(7) Chae, H. K.; Eddaoudi, M.; Kim, J.; Hauck, S. I.; Hartwig, J. F.; O'Keeffe, M.; Yaghi, O. M. *J. Am. Chem. Soc.* **2001**, *123*, 11482.
(8) Gardner, G. B.; Venkataraman, D.; Moore, J. S.; Lee, S. *Nature* **1995**, *374*, 792.
(9) Zheng, N.; Bu, X.; Feng, P. *J. Am. Chem. Soc.* **2002**, *124*, 9688.
(10) Abrahams, B. F.; Hoskins, B. F.; Michail, D. M.; Robson, R. *Nature* **1994**, *369*, 727.
(11) Seward, C.; Jian, W.-L.; Wang, R.-Y.; Enright, G. D.; Wang, S. *Angew. Chem., Int. Ed.* **2004**, *43*, 2933.
(12) Ke, Y.; Collins, D. J.; Sun, D.; Zhou, H.-C. *Inorg. Chem.* **2006**, *45*, 1897.
(13) Lin, X.; Blake, A. J.; Wilson, C.; Sun, X. Z.; Champness, N. R.; George, M. W.; Hubberstey, P.; Mokaya, R.; Schroeder, M. *J. Am. Chem. Soc.* **2006**, *128*, 10745.
(14) Abrahams, B. F.; Jackson, P. A.; Robson, R. *Angew. Chem., Int. Ed.* **1998**, *37*, 2656.
(15) Kitagawa, S.; Masaoka, S. *Coord. Chem. Rev.* **2003**, *246*, 73.
(16) Bu, X. H.; Biradha, K.; Yamaguchi, T.; Nishimura, M.; Ito, T.; Tanaka, K.; Shionoya, M. *Chem. Commun.* **2000**, 1953.
(17) Pang, J.; Marcotte, E. J. P.; Seward, C.; Brown, R. S.; Wang, S. *Angew. Chem., Int. Ed.* **2001**, *40*, 4042.
(18) Shatruk, M.; Chouai, A.; Dunbar, K. R. *Dalton Trans.* **2006**, 2184.
(19) Fourmigué, M.; Uzelmeier, C. E.; Boubekeur, K.; Bartley, S. L.; Dunbar, K. R. *J. Organomet. Chem.* **1997**, *529*, 343.

10.1021/ic061711m CCC: $37.00

**Chart 1**

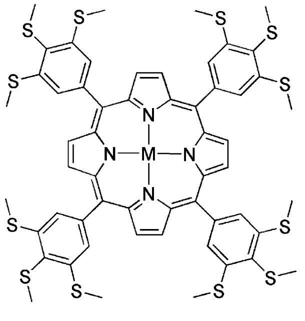

M-T3MTPP (M = Zn, Cu)

5,10,15,20-tetrakis[3′,4′,5′-tris(methylthio)phenyl]porphyrin (Zn-T3MTPP; see Chart 1) with multiple thioether groups symmetrically disposed to hatch chelation links in network formation. We now elaborate on the original aspects of this discovery.

Thioethers (R−S−R′) have proven quite versatile as network building blocks in both the single-fold coordination and the chelation mode.[20−30] In this regard, the symmetric 1,2,3-tris(methylthio)phenyl group presents a versatile multisite donor for forming extended coordination nets. Previously, hexakis(organylthio)benzene or octakis(organylthio)-naphthalene ligands containing the 1,2,3-tris(organylthio) moiety have been used for network formation.[23−25] However, the tris(organylthio) moieties thereof are embedded among other organylthio groups, and their configuration and function as a distinct chelating unit are thus largely obscured. In order to probe and accentuate the utility of the tris(organylthioaryl) moiety as an explicit and prominent chelating unit, we have synthesized ligand Zn-T3MTPP, in which four 1,2,3-tris-(methylthio)phenyl groups are symmetrically affixed onto the metalloporphyrin core. Interestingly, in forming networks with bismuth(III) bromide ($BiBr_3$), an unusually complex chelation link consisting of multiple Bi−S interactions was established across the Zn-T3MTPP ligands, which, in a large connection, is also reminiscent of the multiple hydrogen-bonding motifs that are so widely used in constructing robust supramolecular arrays.

Another potentially important aspect of the discovery here relates to our recent efforts in synthesizing semiconductive coordination networks.[31−33] In the previous networks, significant electronic interactions were observed between $BiX_3$ (X = Cl or Br) components and aromatic $\pi$-electron systems equipped with organylthio (RS−) groups. Besides the substantial charge-transfer phenomena that could lead to potentially useful semiconductive properties, these networks and the other related compounds[34−37] are usually convenient to grow and provide advantages for solution processing. The network herein exemplifies a preliminary effort to install the potentially electroactive bismuth(III)−thioether coordination links across the functional molecular systems of metalloporphyrins. The ultimate prospect of achieving a functional semiconductive network with fully integrated porphyrin units is fascinating because of the rich photophysical and electronic properties associated with the widely studied[10,38−43] porphyrin functionality.

## Experimental Section

Starting materials, reagents, and solvents were purchased from commercial sources (Aldrich and Fisher Scientific) and used without further purification unless stated otherwise. Melting points were measured on a Mel-temp II melting point apparatus and were uncorrected. Solution $^1H$ and $^{13}C$ NMR spectra were recorded on a 200 MHz Varian Mercury spectrometer at room temperature, with tetramethylsilane as the internal standard. Energy-dispersive spectrometry (EDS) was performed on a Philips XL30 FEG scanning electron microscope. The atom ratio of the concerned elements was kept constant in different regions. The results were the average values of three points.

The X-ray datasets of **2** and **3** were collected from red platelike crystals on a Bruker AXS SMART APEX CCD system using Mo K$\alpha$ ($\lambda$ = 0.710 73 Å) radiation. The structure was solved and refined by full-matrix least squares on $F_o^2$ using Bruker Advanced X-ray Solutions *SHELXTL* (version 6.14; Bruker AXS Inc.: Madison, WI, 2003). Selected crystallographic data are summarized in Table 1, with details of the X-ray diffraction studies on the single crystals provided in the Supporting Information.

Powder X-ray diffraction patterns of crystal samples of **2** and **3** (packed inside a sealed capillary) were collected on a Bruker D8 Advance diffractometer with nickel-foil-filtered and monochromatic Cu K$\alpha_{1,2}$ radiation ($\lambda$ = 1.541 t42 Å) operated at 1.6 kW. The primary parallel X-ray beam was generated by a Göbel Mirror and Soller slit (2.5°), and the scattered beam was analyzed by an energy-dispersive X-ray detector (Sol-X) with the following scanning parameters ($2\theta$ range = 5−60°; step size = 0.04°; time per step = 5 s). The sample was continuously rotated during data collection. Deterioration or color change of crystals inside the capillary was

---

(20) Gan, X.; Munakata, M.; Kuroda-Sowa, T.; Maekawa, M. *Bull. Chem. Soc. Jpn.* **1994**, *67*, 3009.

(21) Inoue, M. B.; Inoue, M.; Bruck, M. A.; Fernando, Q. *Chem. Commun.* **1992**, 515.

(22) Zhong, J. C.; Misaki, Y.; Munakata, M.; Kuroda-Sowa, T.; Maekawa, M.; Suenaga, Y.; Konaka, H. *Inorg. Chem.* **2001**, *40*, 7096.

(23) Suenaga, Y.; Kuroda-Sowa, T.; Munakata, M.; Maekawa, M.; Morimoto, H. *Polyhedron* **1998**, *18*, 429.

(24) Suenaga, Y.; Kuroda-Sowa, T.; Maekawa, M.; Munakata, M. *Dalton Trans.* **2000**, 3620.

(25) Suenaga, Y.; Konaka, H.; Kitamura, K.; Kuroda-Sowa, T.; Maekawa, M.; Munakata, M. *Inorg. Chim. Acta* **2003**, *351*, 379.

(26) Li, K.; Xu, Z.; Fettinger, J. C. *Inorg. Chem.* **2004**, *43*, 8018.

(27) Li, K.; Xu, Z.; Xu, H.; Carroll, P. J.; Fettinger, J. C. *Inorg. Chem.* **2006**, *45*, 1032.

(28) Fu, Y.-T.; Lynch, V. M.; Lagow, R. J. *Chem. Commun.* **2003**, 1068.

(29) Fu, Y.-T.; Lynch, V. M.; Lagow, R. J. *Chem. Commun.* **2004**, 1068.

(30) Do, L.; Halper, S. R.; Cohen, S. M. *Chem. Commun.* **2004**, 2662.

(31) Xu, Z.; Li, K.; Fettinger, J. C.; Li, J.; King, M. M. *Cryst. Growth Des.* **2005**, *5*, 423.

(32) Li, K.; Xu, Z.; Xu, H.; Ryan, J. M. *Chem. Mater.* **2005**, *17*, 4426.

(33) Li, K.; Xu, H.; Xu, Z.; Zeller, M.; Hunter, A. D. *Inorg. Chem.* **2005**, *44*, 8855.

(34) Levason, W.; Reid, G. *J. Chem. Soc., Dalton Trans.* **2001**, 2953.

(35) Levason, W.; Orchard, S. D.; Reid, G. *Coord. Chem. Rev.* **2002**, *225*, 159.

(36) Levason, W.; Hill, N. J.; Reid, G. *Dalton Trans.* **2002**, 4316.

(37) Corcoran, S. M.; Levason, W.; Patel, R.; Reid, G. *Inorg. Chim. Acta* **2005**, *358*, 1263.

(38) Pan, L.; Huang, X.; Phan, H.-L. N.; Emge, T. J.; Li, J.; Wang, X. *Inorg. Chem.* **2004**, *43*, 6878.

(39) Carlucci, L.; Ciani, G.; Proserpio, D. M.; Porta, F. *CrystEngComm* **2005**, *7*, 78.

(40) Goldberg, I. *CrystEngComm* **2002**, *4*, 109.

(41) Goldberg, I. *Chem. Commun.* **2005**, 1243.

(42) Suslick, K. S.; Bhyrappa, P.; Chou, J. H.; Kosal, M. E.; Nakagaki, S.; Smithenry, D. W.; Wilson, S. R. *Acc. Chem. Res.* **2005**, *38*, 283.

(43) Boyd, P. D. W.; Reed, C. A. *Acc. Chem. Res.* **2005**, *38*, 235.

**Table 1.** Selected Crystallographic Data for **2** and **3**

| | **2** | **3** |
|---|---|---|
| chemical formula | $C_{104}H_{96}Bi_4Br_{12}N_8$-$O_8S_{12}Zn$ | $C_{104}H_{96}Bi_4Br_{12}N_8$-$O_8S_{12}Cu$ |
| fw | 3830.84 | 3828.99 |
| space group | $P2_1/n$ | $P2_1/n$ |
| $a$, Å | 13.894(2) | 13.949(2 |
| $b$, Å | 27.684(5) | 27.592(4) |
| $c$, Å | 16.744(3) | 16.714(2) |
| $\beta$, deg | 106.879(3) | 107.134(2) |
| $V$, Å$^3$ | 6163(2) | 6147(1) |
| $Z$ | 2 | 2 |
| $\rho_{calcd}$, g/cm$^3$ | 2.064 | 2.069 |
| wavelength, Å | 0.710 73 (Mo Kα) | 0.710 73 (Mo Kα) |
| abs coeff ($\mu$), mm$^{-1}$ | 10.032 | 10.035 |
| R1[a] | 3.10% [$I > 2\sigma(I)$] | 2.57% [$I > 2\sigma(I)$] |
| wR2[b] | 7.56% [$I > 2\sigma(I)$] | 5.66% [$I > 2\sigma(I)$] |

[a] $R1 = \Sigma||F_o| - |F_c||/\Sigma(|F_o|)$. [b] $wR2 = \{\Sigma[w(F_o^2 - F_c^2)^2]/\Sigma[w(F_o^2)^2]\}^{1/2}$.

not observed after data collection. Diffraction data of **2** were corrected by the background contribution and sample displacement error, and the corrected and scaled data were compared with that generated by a simulation program *Mercury 1.4*, which was based on single-crystal data of the sample (see the Supporting Information for the patterns). Crystals of **2** and **3** display similar diffraction patterns in the same spectral range as that of the isostructural analogues.

**3,4,5-Tris(methylthio)benzaldehyde (1).** In an argon-filled glovebox, sodium methylthiolate (3.32 g, 95%, 45.0 mmol) and a magnetic stirring bar were loaded into a two-neck round-bottomed flask. The flask was then taken out of the glovebox and connected to a nitrogen bubbler. DMEU (anhydrous, 50 mL) was transferred via a cannula into the flask, and stirring was started. 3,4,5-Trifluorobenzaldehyde (1.61 g, 99%, 10 mmol) dissolved in DMEU (anhydrous, 30 mL) was purged with nitrogen for 5 min and then transferred into the flask slowly at room temperature. After being stirred at room temperature for 20 min, the mixture changed into a red-brown solution. At 1 h, methyl iodide (3.4 mL, 99%, 53.9 mmol) was injected slowly into the solution when the mixture was chilled in an ice/water bath. The resultant light-yellow solution was poured into water (100 mL), and the aqueous suspension was extracted with hexanes/dichloromethane (1:1, 100 mL × 3). The organic layers were combined and washed with water (200 mL × 3) and brine (200 mL). After being dried over anhydrous sodium sulfate for 10 min, the solvent was removed on a rotary evaporator to afford a yellow solid. The crude product was purified by flash chromatography (with 1:2 $CH_2Cl_2$/hexanes as the eluent) to yield the pure product as a light-yellow solid (1.55 g, 63% based on the starting trifluorobenzaldehyde). Mp: 150−152 °C. $^1H$ NMR (200 MHz, $CD_2Cl_2$): $\delta$ 2.36 (s, 3 H), 2.49 (s, 6 H), 7.32 (s, 2 H), 9.97 (s, 1 H). $^{13}C$ NMR (50 MHz, $CD_2Cl_2$): $\delta$ 15.78, 17.26, 120.00, 134.79, 137.18, 148.84, 191.77.

**2*H*-5,10,15,20-Tetrakis[3′,4′,5′-tris(methylthio)phenyl]porphyrin (2*H*-T3MTPP).** To an oxygen-free solution of 3,4,5-tris(methylthio)benzaldehyde (1.07 g, 4.4 mmol) in dichloromethane (anhydrous, 290 mL) was added pyrrole (0.30 g, 99%, 4.4 mmol, purged with nitrogen for 5 min) under nitrogen protection. After 5 min, boron trifluoride diethyl etherate (0.1 mL, 1 M in dichloromethane) was injected at room temperature while the mixture was stirred magnetically. The mixture was then covered with aluminum foil, and the stirring was continued for another 2 h, followed by the addition of *p*-chloranil (2,3,5,6-tetrachloro-1,4-benzoquinone, 0.81 g, 99%, 3.3 mmol) into the resultant dark-red-brown solution. The burgundy mixture was then heated to reflux for 1 h. After being cooled down to room temperature, the mixture was transferred into a round-bottomed flask and silica gel was added. After removal of the solvent in vacuo, the purple residue was loaded on top of a prepacked silica gel column. The column was then eluted first with 50% (by volume) dichloromethane in hexanes to remove the side products. The product was then eluted by 70% dichloromethane in hexanes. After evaporation of the solvent in vacuo, the pure product was obtained as a shiny purple solid [0.54 g, 42% based on 3,4,5-tris(methylthio)benzaldehyde]. Mp: 398−400 °C. $^1H$ NMR (200 MHz, $CDCl_3$): $\delta$ 2.42 (s, 24 H), 2.67 (s, 12 H), 7.72 (s, 8 H), 8.96 (s, 8 H). $^{13}C$ NMR (50 MHz, $CDCl_3$): $\delta$ 15.97, 17.83, 119.84, 126.17, 128.03, 131.16, 131.54, 143.67, 145.56.

**Zinc(II) 5,10,15,20-Tetrakis[3′,4′,5′-tris(methylthio)phenyl]porphyrin (Zn-T3MTPP).** A stirred mixture of 2*H*-T3MSPP (0.21 g, 0.18 mmol) and zinc acetate dihydrate (42 mg, 99%, 0.19 mmol) in dimethylformamide (DMF; 30 mL) was refluxed for 15 min before water (150 mL) was added and the resultant suspension/emulsion extracted with dichloromethane (100 mL × 3). The combined organic layers were washed with water and brine and dried over sodium sulfate for 15 min. After removal of the solvent on a rotary evaporator, the product was obtained as a purple solid. The crude product was purified by a short column with 3:2 $CHCl_3$/hexanes as the eluent (0.18 g, 84% based on 2*H*-T3MTPP). Mp: 385−387 °C (without dec). $^1H$ NMR (200 MHz, $CDCl_3$): $\delta$ 2.41 (s, 24 H), 2.68 (s, 12 H), 7.71 (s, 8 H), 9.06 (s, 8 H). $^{13}C$ NMR is not available because of low solubility in common deuterated solvents. Further characterization was provided by the subsequent single-crystal X-ray diffraction analysis of the hybrid extended networks (see below) prepared from this compound.

**Copper(II) 5,10,15,20-Tetrakis[3′,4′,5′-tris(methylthio)phenyl]porphyrin (Cu-T3MTPP).** By refluxing of a mixture of 2*H*-T3MTPP (0.17 g, 0.14 mmol) and copper(II) chloride (42.6 mg, 99.5%, 0.32 mmol) in DMF (15 mL) for 2 h, Cu-T3MTPP was prepared in 82% yield (0.15 g after flash column separation with 3:2 $CHCl_3$/hexanes as the eluent) as a red-purple solid. Mp: 379−380 °C. NMR is not available because of low solubility in common deuterated solvents. Further characterization was provided by the single-crystal X-ray diffraction analysis of the hybrid extended networks prepared from this compound.

**X-ray-Quality Single Crystals of 2.** Inside an argon-filled glovebox, a nitrobenzene solution of Zn-T3MTPP (0.4 mL, 1.68 mM) was layered at the bottom of three glass tubes (10 mm o.d./6 mm i.d.). A 1:1 mixture of nitrobenzene/benzene (0.2 mL) and a benzene solution of $BiBr_3$ (6.7 mM, 0.2, 0.4, and 0.6 mL, respectively) were layered sequentially without disturbing the interfaces. The tubes were sealed with Parafilm and left upright and undisturbed inside the glovebox. After about 7 days, red platelike single crystals suitable for X-ray diffraction analysis were observed for the setups with 0.4 and 0.6 mL of $BiBr_3$ solution (i.e., with ligand/$BiBr_3$ ratios at 1:4 and 1:6, respectively). Single-crystal X-ray diffraction analysis for both batches of crystals yielded the same crystal structure of **2**. Powder X-ray diffraction studies indicated a single phase consistent with the single-crystal structure (see Figure S5 in the Supporting Information). EDS (by a Philips XL30 FEG scanning electron microscope) measurement of the product indicated the S/Zn/Bi/Br ratio to be 11.7:1.0:3.9:9.5. The crystal growth experiments are readily repeatable, and exact yields will be obtained in subsequent preparations on larger scales. A similar procedure was used for obtaining the single crystals of **3**.

**Scheme 1**[a]

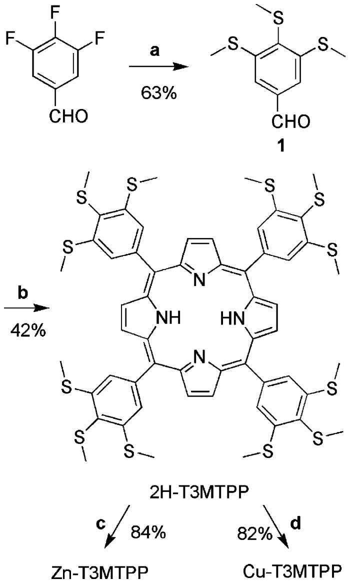

[a] Key: (a) NaSMe, DMEU, rt, $N_2$, 1 h, MeI; (b) pyrrole, $CH_2Cl_2$, $BF_3$ etherate, $N_2$, rt, 2 h/*p*-chloranil, reflux, 1 h; (c) $Zn(AcO)_2$, $CHCl_3$, reflux, 1 h; (d) $CuCl_2$, DMF, reflux, 2 h.

## Results and Discussion

The metalloporphyrin ligands Zn-T3MTPP and Cu-T3MTPP were efficiently synthesized in a multistep procedure (see Scheme 1). The reaction of sodium methylthiolate with 3,4,5-trifluorobenzaldehyde gave in 63% yield of **1**. In comparison to the reported multistep synthetic route to **1**,[44] this single-step procedure provides obvious advantages. Aldehyde **1** was then subjected to the Lindsey porphyrin synthesis conditions[45] to afford 2*H*-T3MTPP as the product in 42% yield. The metalation of the porphyrin thus obtained was carried out by refluxing of the porphyrin with a metal salt [$Zn(OAc)_2$ or $CuCl_2$] in DMF, and the processes were usually complete in 2 h. The purification was straightforward (usually by a short silica gel flash column), and yields were good (see the Experimental Section for details).

The crystallization of the Zn-T3MTPP (or Cu-T3MTPP) ligand with $BiBr_3$ was conducted at room temperature in a slow-diffusion setup (see the Experimental Section). X-ray structure determination on the resultant single crystals indicated a chemical composition of Zn-T3MTPP·4$BiBr_3$·4$PhNO_2$·4benzene (**2**). An isomorphic product (**3**) was obtained with Cu-T3MTPP (detailed crystallographic data for **2** and **3** are given in the Supporting Information). The composition of **2** is also consistent with the results from thermogravimetric analysis (TGA) measurement. As seen in Figure S1 in the Supporting Information, the thermogram of the solid sample of **2** features a distinct step of weight loss of about 20% around 120 °C, corresponding to the removal of the included benzene and nitrobenzene molecules (calculated weight percentage of benzene and nitrobenzene in **2**: 21.0%). Powder X-ray diffraction studies indicate that the evacuation of guest molecules resulted in a substantial loss of the crystalline order of the original frameworks. Further studies are ongoing for obtaining more robust frameworks.

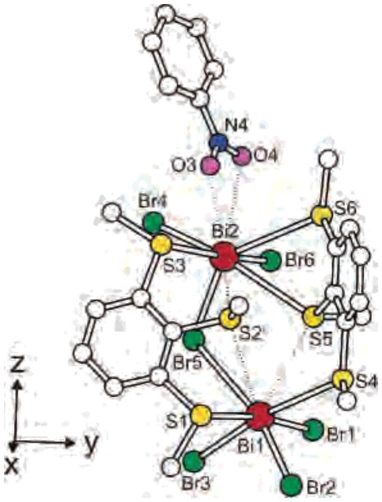

**Figure 1.** Chelation motif in the crystal structure of **2**. Interatomic distances (Å): Bi1−Br1, 2.6735(5); Bi1−Br2, 2.6519(5); Bi1−Br3, 2.6449(5); Bi1−Br5, 3.378; Bi1−S1, 3.085(1); Bi1−S2, 3.630(1); Bi1−S4, 3.3394(9); Bi1−S5, 3.428(1); Bi2−Br4, 2.6243(5); Bi2−Br5, 2.6785(6); Bi2−Br6, 2.6457-(6); Bi2−S2, 3.590(1); Bi2−S3, 3.264(1); Bi2−S5, 3.326(1); Bi2−S6, 3.337(1); Bi2−O3, 3.112(4); Bi2−O4, 3.116(3). Bi−S and Bi−Br interactions above 3.4 Å and Bi−O interactions are shown as dotted lines.

The crystal structure formed in the space group $P2_1/n$ ($a = 13.894$ Å, $b = 27.684$ Å, $c = 16.744$ Å, and $\beta = 106.879°$), with the asymmetric portion of the unit cell containing half of the Zn-T3MTPP molecule and two $BiBr_3$ fragments, together with two benzene molecules and two nitrobenzene molecules included as guest molecules. The Zn-T3MTPP molecule adopts a centrosymmetric conformation with the pendant phenyl groups significantly tilted out of the plane with the porphyrin core (dihedral angles: 75 and 63°). The interaction of the Zn-T3MTPP ligand with the $BiBr_3$ components is established primarily through the coordination between the $Bi^{III}$ center and the S atoms on the ligand. The local bonding features are shown in Figure 1, in which three distinct components can be identified as the $Bi_2Br_6$ portion, two tris(methylthio)phenyl groups (from two neighboring Zn-T3MTPP molecules), and one associated nitrobenzene molecule. The $Bi_2Br_6$ unit is based on the sharing of the Br5 atom, which interacts with Bi1 and Bi2 in rather different interatomic distances (Bi1−Br5, 3.38 Å; Bi2−Br5, 2.68 Å). Additionally, Bi1 further bonds to three Br atoms (Br1, Br2, and Br3), while Bi2 bonds to only two (Br4 and Br6). Part of the remaining coordination sphere of Bi2 is occupied by the two O atoms of a nitrobenzene molecule featuring Bi−O distances of 3.11 and 3.12 Å.

One striking feature of the current network is the multiplicity of the chelation interactions in the linkage across the neighboring ligands; namely, the $Bi_2Br_6$ unit serves as a complex Lewis acid linkage and forms a relatively large number of coordination bonds and secondary interactions with the neighboring Zn-T3MTPP molecules. As shown in Figure 1, the interatomic distances are quite variable, as is typical of secondary interactions in other systems.[46,47] For one of the tris(methylthio)phenyl groups, the major links are

---

(44) Kompis, I.; Wick, A. E. Patent DE2847825, 1979.

(45) Lindsey, J. S.; MacCrum, K. A.; Tyhonas, J. S.; Chuang, Y. Y. *J. Org. Chem.* **1994**, *59*, 579.

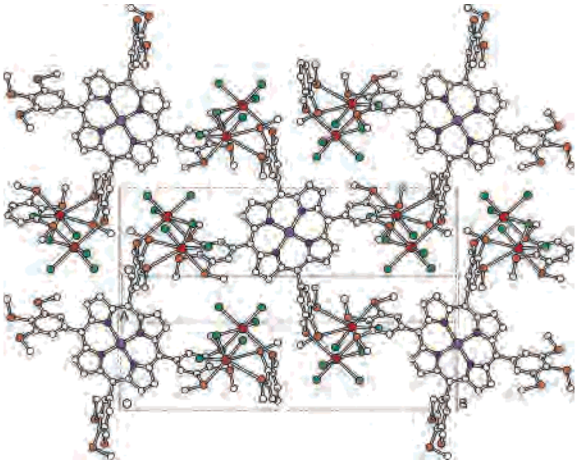

**Figure 2.** 2D net in **2**. Color code: large red sphere, Bi; large purple sphere, Zn; medium green sphere, Br; medium orange sphere, S; small white sphere, C; small blue sphere, N.

Bi1−S1 (3.09 Å) and Bi2−S3 (3.26 Å); for the other, they are Bi2−S5 (3.33 Å), Bi2−S6 (3.34 Å), Bi1−S4 (3.34 Å), and Bi1−S5 (3.43 Å). In addition, atom S2 also interacts with Bi1 and Bi2 at longer distances (3.63 and 3.59 Å, respectively). Such multiple-fold chelation interactions between neighboring ligands are rare among the coordination networks because most networks are based on only one or two coordination bonds between the ligating unit (e.g., $-COO^-$, $-CN$) and metal centers. This multiple-coordination motif is also reminiscent of the multiple hydrogen-bonding patterns that are widely used for strengthening supramolecular networks and may similarly serve as a possible means for reinforcing the coordination linkages across the organic ligands. Further study is ongoing in this group to probe the generality and utility of similar multiple-interaction patterns for assembling functional coordination networks.

The network thus resulting from the intermolecular linkage is two-dimensional, and an overview of the net is depicted in Figure 2. The connectivity of the network can be represented by connecting the Zn atom (as the center of the Zn-T3MTPP ligand) and the geometric center of the interlinking $Bi_2Br_6$ block (roughly treated as the midpoint between the two Bi atoms). The resultant representation is a relatively simple four-connected net as shown in Figure 3. The 2D net is parallel to the lattice plane [−1, 0, 1]. The 2D network shows substantial corrugation, and large void space exists between the neighboring networks (see Figures S2 and S3 in the Supporting Information). The void space is occupied by the nitrobenzene and benzene molecules from the crystallization process (see Figure S4 in the Supporting Information). Among the two crystallographically equivalent nitrobenzene molecules, one is coordinated to the Bi2 atom and the other is stacked parallel to the metalloporphyrin core, with an interplanar distance of 3.33 Å. Because of the centrosymmetric packing in the structure, each porphyrin core is thus sandwiched by two crystallographically equivalent nitrobenzene guests. By comparison, the interaction of the benzene molecules with the host network is less distinct, and they appear to function mostly as van der Waals space fillers.

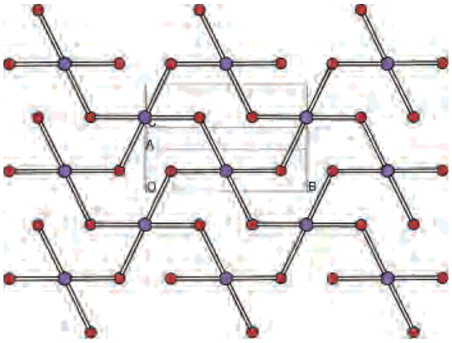

**Figure 3.** Topological representation of the 2D net in **2**. Color code: purple sphere, Zn; red sphere, midpoint of Bi1 and Bi2 in the $Bi_2Br_6$ unit.

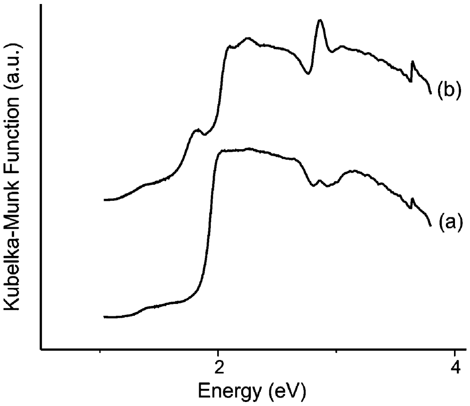

**Figure 4.** Room-temperature solid-state absorption spectra for (a) Zn-T3MTPP and (b) **2**.

It has been in our interest to observe the potential electronic interaction between the metalloporphyrin core and the $BiBr_3$ component within this composite network because our previous work has established that effective electronic interactions could be achieved between large aromatic hydrocarbon ligands and $Bi^{III}$ centers. Diffuse-reflectance measurements were therefore carried out on the solid samples of Zn-T3MTPP and network compound **2**. As shown in Figure 4, compound Zn-T3MTPP features a major absorption at about 1.9 eV, corresponding to the Q band in typical molecular metalloporphyrin systems. The Q-band feature continues to dominate in the spectrum of compound **2**, indicating the distinct contribution from the porphyrin moiety. Notably, a slightly red-shifted new absorption feature occurs at 1.8 eV, which might be ascribed to the electronic interaction between the $Bi_2Br_6$ fragment and the porphyrin core. In comparison with the dominant red shift of the previously studied aromatic hydrocarbon systems,[32,33] the new absorption feature of **2** appears quite modest, suggesting weaker electronic coupling between the ligand and the $BiBr_3$ component. The weaker electronic coupling might partly be due to the nonplanar alignment of the porphyrin core and the pendant phenyl groups of Zn-T3MTPP. We also suspect that the highest occupied molecular orbital level of the metalloporphyrin molecule is lower than that of the previously studied aromatic hydrocarbon systems, hindering the electron donation onto the Lewis acid units of $BiBr_3$. Further

---

(46) Starbuck, J.; Norman, N. C.; Orpen, A. G. *New J. Chem.* **1999**, *23*, 969.
(47) Alcock, N. W. *Adv. Inorg. Chem. Radiochem.* **1972**, *15*, 1.

study is ongoing to access systems for stronger electronic interaction that more effectively integrates the porphyrin core into a semiconductive coordination network.

## Conclusion

In short, we have explored the usefulness of the 1,2,3-tris(methylthio)phenyl group as a distinct and prominent chelating unit in forming functional coordination networks. The porphyrin-based networks reported herein could serve as a first step toward semiconductive coordination networks in which the porphyrin unit is more fully integrated via stronger electronic interactions. In a wider perspective, the methyl groups could be replaced by more sophisticated organic groups, the resultant tris(organylthio)phenyl unit could be attached to a variety of building blocks, and a variety of other metal salts could be used as acceptors, in order to explore other patterns of multiple chelation links and to achieve crystalline networks with more advanced functions and properties.

**Acknowledgment.** This work is partially supported by City University of Hong Kong (Project No. 9360121) and by a grant from the Research Grants Council of the Hong Kong Special Administrative Region, China [Project No. 9041109 (CityU 102406)]. We thank the donors of the American Chemical Society Petroleum Research Fund for partial support of this research, and one of the diffractometers was funded by NSF Grant 0087210, by the Ohio Board of Regents Grant CAP-491, and by Youngstown State University. We also thank Dr. Yanqiong Sun for demonstrating further the repeatability of the crystal growth.

**Supporting Information Available:** Full crystallographic data in CIF format for **2** and **3**, a TGA plot for the solid sample of **2**, additional figures of the crystal structure of **2**, and powder X-ray diffraction patterns of **2**. This material is available free of charge via the Internet at http://pubs.acs.org.

IC061711M